



# Comparative analysis of groundwater potentiality zone using fuzzy AHP, frequency ratio and Bayesian weights of evidence methods

Biswajit Maity<sup>1</sup> · Suraj Kumar Mallick<sup>1</sup> · Pritiranjana Das<sup>1</sup> · Somnath Rudra<sup>1</sup>

Received: 1 September 2021 / Accepted: 9 February 2022 / Published online: 9 March 2022  
© The Author(s) 2022

## Abstract

Groundwater resource management in the urban area is one of the important aspects because of growing population demand and having inadequate water supply. So, proper information is needed to manage the future urban planning for such kinds of areas. This study emphasizes groundwater potentiality zone (GPZ) assessment in the Asansol urban agglomeration (AUA) region, West Bengal, India. For this purpose, we have incorporated eight conditioning factors namely LULC, lithology, slope, elevation, rainfall, drainage density, lineaments density, and soil map using conventional and remote sensing data in GIS software. All these conditioning factors have been reclassified in ArcGIS and processed by the fuzzy analytical hierarchy process (FAHP), frequency ratio (FR), and Bayesian weights of evidence (BWOE) statistical methods. Then, the groundwater potential index has been formulated, and finally, GPZ maps are generated based on of selected three models. The result shows that very high area of GPZ, e.g. 9.13%, 11.62% and 7.43% are under BWOE, FR and FAHP models, respectively. The receiver operating characteristic validation curves show that FR method (AUC = 96.4%) is well obtained for GPZ in comparison with both BWOE (AUC = 83.8%) and FAHP methods (AUC = 82.9%). Therefore, this statistical method is highly recommended for the study of groundwater potential assessment and this outcome is very suitable for the groundwater resources management in future land use planning. Precautionary works in low potential areas should be given priority for long-term planning. Thus, this study can be considered as a good document for decision support in water exploitation planning and sustainable groundwater management in AUA region.

**Keywords** Asansol urban agglomeration · Groundwater potentiality · Fuzzy analytical hierarchy process · Frequency ratio · Bayesian weights of evidence

## Introduction

Groundwater is one of the precious entities in nature that occupying the pore and fracture space under the geological stratum (Naghibi et al. 2015). It plays a significant role in terms of environmental, economic and human wellbeing throughout the world (IPCC 2001; Mallick et al. 2019). About 30% of the world freshwater is reserved as groundwater, whereas surface water contributes only 0.3% of freshwater (Senanayake et al. 2016). Since the last century, the demand for freshwater is immensely increasing due to the agricultural revolution, industrialization, and urbanisation (Manap et al. 2014). According to the

census of India, in 1991, about 1/10 people lived in urban areas but now (2011) it has become 1/3 (Chandramouli and General 2011). The increasing trends of urbanisation create an impact on the quantity and quality of available groundwater in various ways such as low recharge due to soil sealing, water shortage due to increasing demand, point and a non-point source of water pollution (Rogers 1994; Strohschon et al. 2013; Jha, Singh and Vasta 2008; Wakode et al. 2018; Mallick et al. 2021a). Consequently, the proper supply of clean and fresh water has become a challenging issue. Near future urban areas have to be self-sustain in water through proper management of water supply and consumption. The most exigent part of groundwater resources management and protection are to map and delineate the groundwater recharge potential (Pathak 2017; Chen et al. 2018). The groundwater potential aquifer has supplied good quality water to the urban areas throughout the year (Singh et al. 2013). So, GPZ

✉ Somnath Rudra  
rudra347@rediffmail.com

<sup>1</sup> Department of Geography, Vidyasagar University,  
Midnapore, India

delineation is a prerequisite to identify the site suitability for the future urban residential zone (Mallick and Rudra 2021a). The availability of groundwater in any region is influenced by the interaction among hydrogeological, climatic and biological factors (Das 2019). Hence, geology, slope, topographical and lithological variation, elevation, soil type, drainage, and lineament, rainfall, distance from the river, land use and land cover, etc. identify the groundwater store and movement under the geological stratum (Ozdemir 2011; Rahmati et al. 2014; Tiwari et al. 2019; Oh et al. 2011; Mallick et al. 2014).

The invention of integrated remote sensing (RS) and GIS techniques is now a paradigm shift in groundwater exploration research through accurate access and monitoring. The satellite-based RS techniques have provided freely, accurate and neutral data about the earth surface, which helps to create the attribute data layer for delineating GPZ. GIS-based multi-criteria analysis, geo-information techniques, and integrated multi-criteria decision analysis (MCDA) are very useful methods for decision making for problems involving too many influencing factors in identifying groundwater recharge zone (Machiwal et al. 2011; Kumar et al. 2014; Fenta et al. 2015; Singh et al. 2017). Besides the GIS-based weighted overlay analysis using thematic maps, several statistical approaches like analytic hierarchy process (AHP) (Shekhar and Pandey 2015; Rahmati et al. 2015), frequency ratio (FR) (Oh et al. 2011; Elmahdy and Mohamed 2015; Zeinivand and Nejad 2018), fuzzy analytic hierarchy process (FAHP) (Aryafar et al. 2013; Sener et al. 2018; Mallick and Rudra, 2021a), certainty factor (Razandi et al. 2015) and Bayesian weights of evidence (BWOE) (Al-Abadi 2015; Chen et al. 2018; Kordestani et al. 2019) are also used to delineate the GPZ for better representation. These methods can be validated through ROC curves (Mallick and Rudra, 2021a).

The Asansol urban agglomeration (AUA) becomes an economic and industrial hub and the second largest urban agglomeration of West Bengal (Maity et al. 2020). Consequently, the population pressure and urban built-up area are increasing rapidly in these cities (Shikary and Rudra 2020; Maity et al. 2021). As this is a mining and industrial region, water supply and management will be a challenging issue in future. Therefore, the aim of this research is to delineate the groundwater potentiality zone for sustainable urban planning. In this regard, this study ensemble fuzzy AHP, FR, and BWOE models to get better results than single models, while delineating groundwater potentiality zones based on eight thematic layers, e.g. DEM, slope, drainage density, lineament density, soil, lithology, rainfall, and LULC, that could have served water resource planners, decision-makers, and urban planners for proper urban planning and sustainable use of water resources.

## Study area

Asansol region is one of the significant urban bodies in West Bengal in terms of economic activities and urbanisation. Consequently, the landscape pattern has been changed within the last few decades. Recently, this study area took the attention of the urban geographer. Asansol urban agglomeration, which lies in 23°34'30" N to 23°48'00" N and 86°8'00" E to 87°8'00" E (Fig. 1), is consisting of 3 municipalities and 1 Municipal corporation covering an area of about 461.20 km<sup>2</sup>, and 11.5 lakhs population. Physio-graphically, this area is located in the lower part of Chotanagpur Plateau on the left bank of Damodar River with an average elevation of 111 m from mean sea level and it consists of the meta-sedimentary rocks of Precambrian age, Gondwana sedimentary rocks, Rajmahal basalts, and upper tertiary sediments. This area has coarse gritty soil blended with rock fragments that are formed from the weathering of pegmatite, quartz veins, and conglomeratic sandstones, whereas sandy, Red, and Yellow Ultisols soil with low in nitrogen, calcium, phosphate, and mineral resource such as coal, iron ores, calcium carbonate, abrasives, silica bricks, glass sands, building materials, moulding sands, manganese, bauxite, laterite, etc. are found in this region. A very mixed types of natural vegetation are found in this region like *Sal* (*Shorea robusta*), *Palas* (*Butea monosperma*), *Mohua* (*Madhuca longifolia*), *Kendua* (*Diospyros melanoxylon*), *Shirisha* (*Albizia lebbek*), *Bans* (*Bambusa arundinacea*), *Arka* (*Calotropis gigantea*), *Arjun* (*Terminalia arjuna*) and *Ashan* (*Tilia tomentosa*). The climate of this region is tropical savanna types. The April to June months are the warmest month and December to February months are the coolest month with a mean annual temperature is 26.2 °C and mean annual rainfall is 1430 mm.

## Materials and methods

### Database

To examine the groundwater potentiality zone (GPZ), various types of data are used and acquired from different sources. Rainfall data have been collected from the Indian Meteorological substation in Asansol. The cloud-free satellite images from multi-spectral Landsat -8 (OLI/TIRS) and Digital Elevation Model (DEM) have been acquired from the United States Geological Survey (USGS) (<http://earthexplore.usgs.gov>). All the detailed specifications of the satellite images are shown in Table 1. The soil samples collection and the location of existing wells are identified

**Fig. 1** Location map of Asansol urban area along with Bore well sites

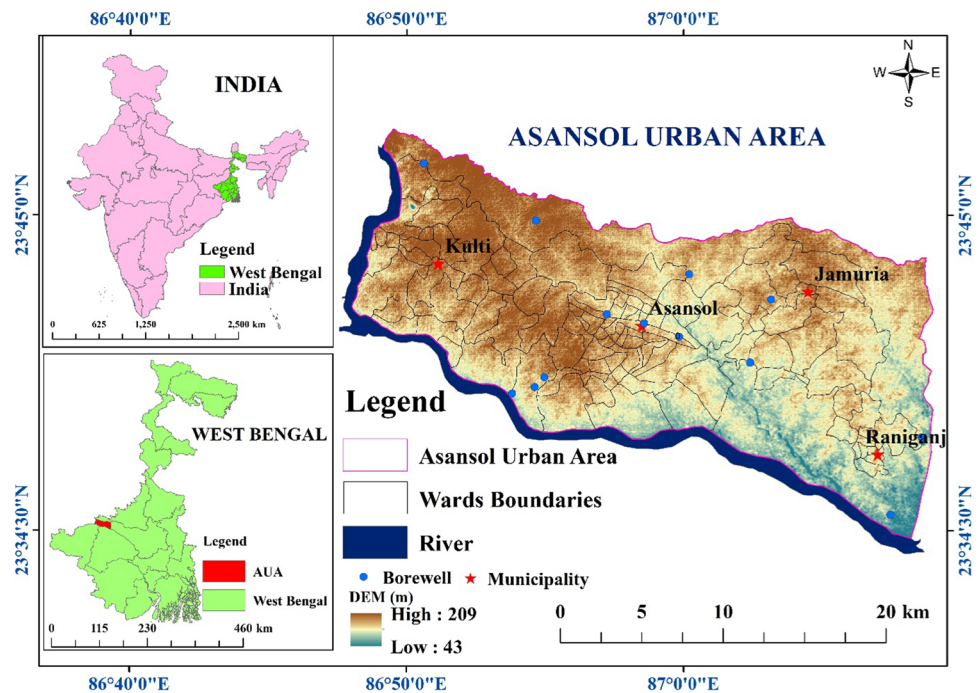


**Table 1** Specifications of the satellite imageries

Acquisition date	Satellite	Path/row	Resolution	Referencing system
23/11/2020	Landsat-8 OLI	139/43	30 m, 100 m (b-10, 11), 15 m (b-8)	UTM 45°N and WGS 84
15/03/2011	ASTER DEM	NA	30 m	

from different sites of the study area during field surveys using GPS. The laboratory experiment of these soil samples has been done for grain size distribution and permeability. The data processing of the whole study was done by ArcGIS, ENVI, MS-office, and SPSS software. All the methods used in this study have been indicated in Fig. 2.

**Data processing for groundwater potential zones mapping using GIS**

In order to evaluate the groundwater potentiality zone of Asansol Urban Area (AUA), eight thematic maps, namely LULC, lithology, slope, elevation, rainfall, drainage density, lineaments density, and soil characteristics, have been generated using conventional and remote sensing data in GIS software.

**Land use/land cover (LU/LC)**

Globally, anthropogenic activities (directly or indirectly) are responsible for damage to the environment such as groundwater depletion, deforestation, soil erosion, and loss of soil quality. Land use/land cover change is one of the crucial

factors for the change of groundwater. In this study, supervised land use/land cover classification has been done by using the Gaussian Maximum Likelihood Classifier Algorithm (GMLCA) in ArcGIS (v.10.1) software. The classification result has been validated through Kappa coefficient. As a result, the six different LULC classes (Fig. 4.h) have been found and the proportionate share of each class is about agricultural land (36.85%), built-up area (21.20%), dry/barren land (28.20%), mining and industrial area (4.91%), vegetation cover (7.20%), and waterbodies (1.65%). Consequently, with the increasing trend of urban areas, groundwater availability becomes a question to the Asansol urban area.

**DEM**

The groundwater prospects are likely to be affected by topographic elevation and regulated by various hydrogeological and geomorphological processes. The topographical elevation in this study has been developed by the digital elevation model (DEM) (Fig. 3a) and extracted from ASTER DEM data. The higher elevation is found in the north-western part and the lower elevation is found in the south and south-eastern part of AUA along the Damodar Riverbank. For

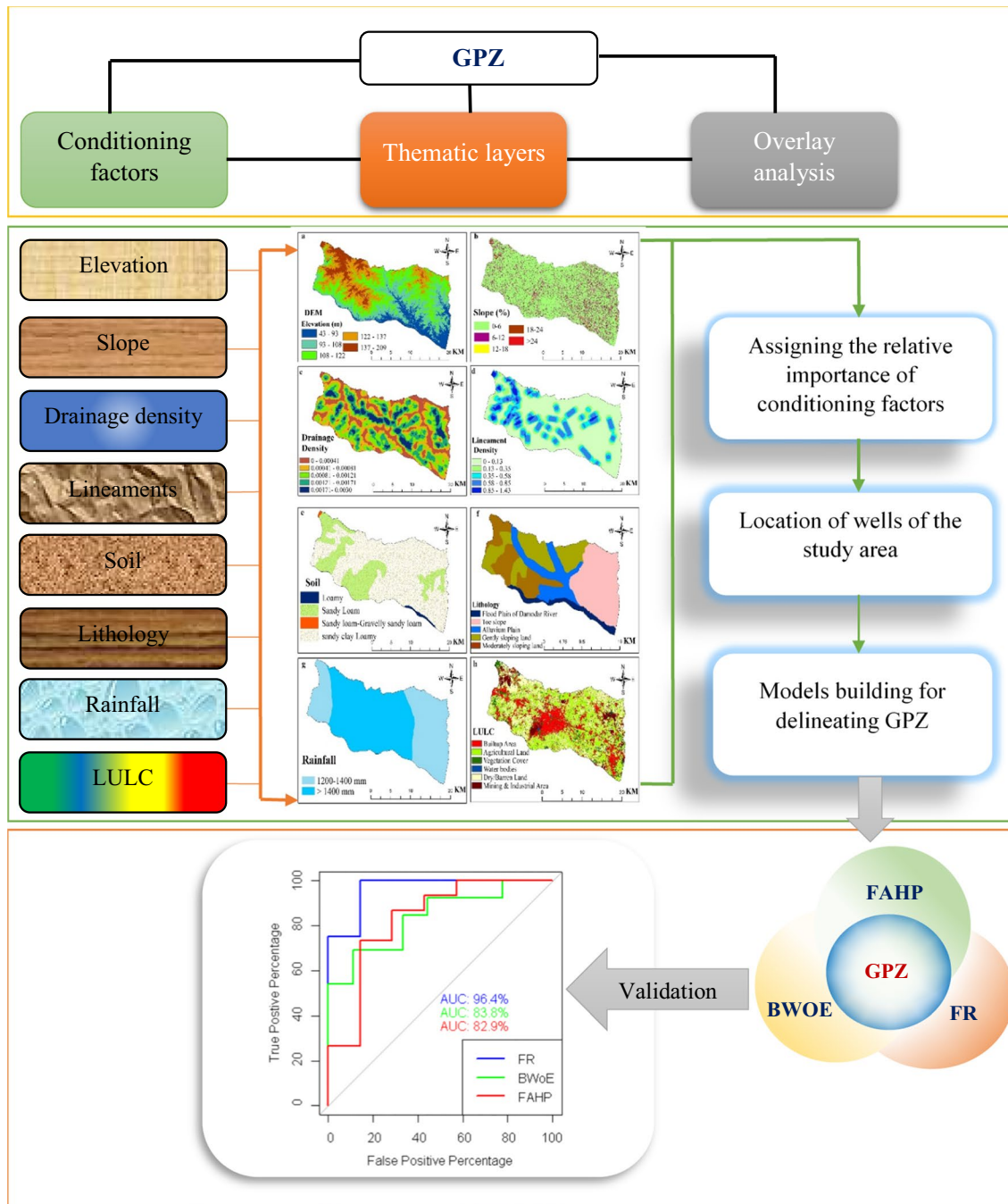


Fig. 2 Methodological flowchart of this study

delineating the GWPZ, higher weight is assigned for lower elevation and vice versa.

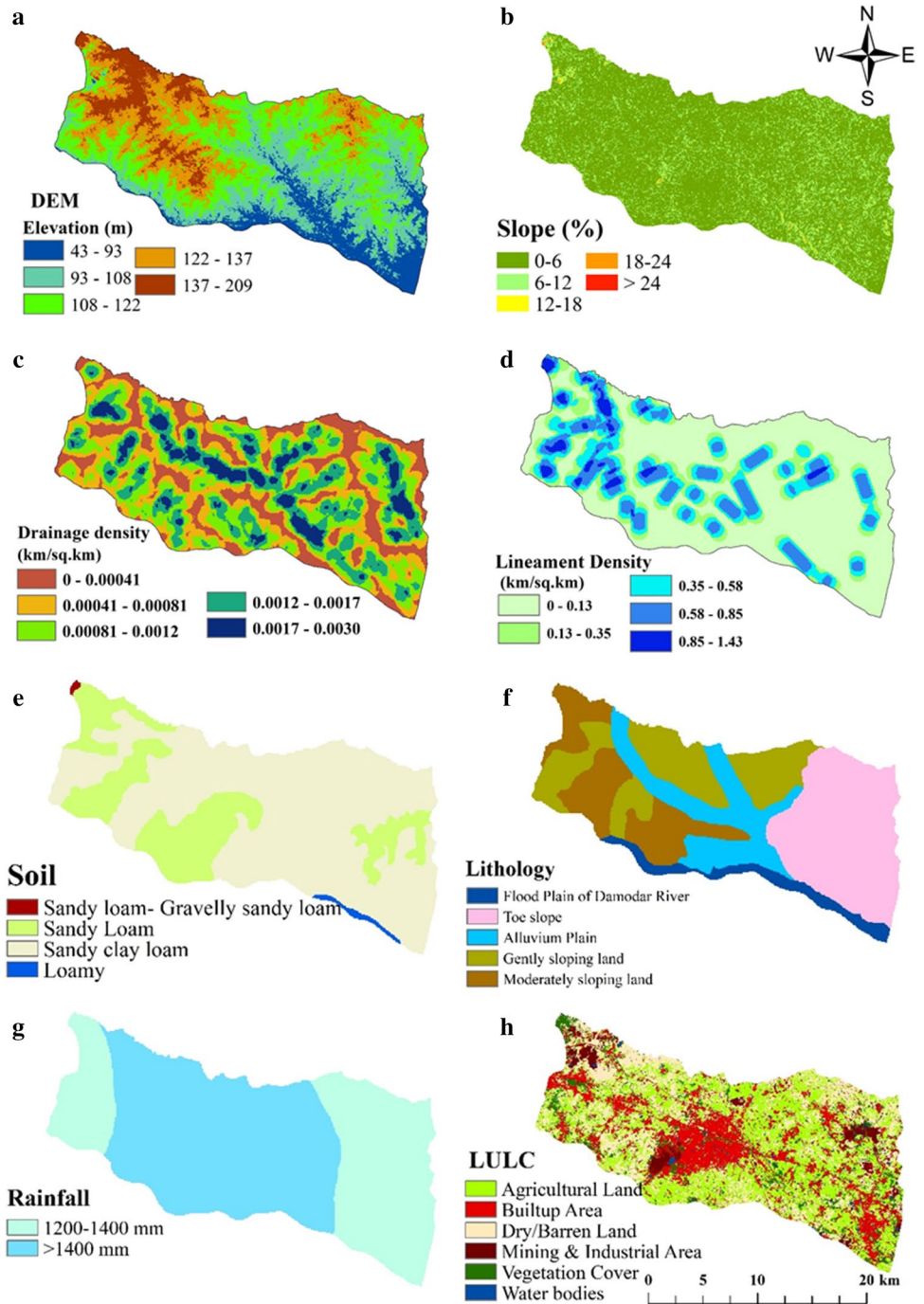
**Slope**

The availability and flow of groundwater are highly controlled by the slope (Yeh et al. 2016). The slope was derived from ASTER DEM data of AUA (Fig. 3b). In this study, the slope has been reclassified into five classes

according to the value of slope (Boughariou et al. 2021) and represented by percentage value. The slope area of 0–6% is covering almost entire area, which refers to the gentle slope in the favour of highest rate of infiltration and 6–12%, 12–18%, 18–24% and > 24% covering the remaining part of the study area. The infiltration rate of surface water into subsurface water is high in gentle slope area which allows more time to percolate and vice versa. (Das et al. 2019).



**Fig. 3** Selected thematic layers for the analysis of groundwater potentiality



**Lineaments Density**

The lineaments are the area of weakness surface with some linear to curvilinear features in the geological structure, such as fracture, fault, and joint. The groundwater intensity is highly influenced by the lineament density (Al-Ruzouq et al. 2019; Yeh et al. 2016). The geological map was used to extract the lineament density in this study. The high weight assigned for high lineament density represents the high recharge zone and vice versa. In this study, five

lineament density zones (Fig. 3d) were identified which are 0–0.13 (very low), 0.13–0.35 (low), 0.35–0.58 (moderate), 0.58–0.85 (high), 0.85–1.43 km/km<sup>2</sup> (very high).

**Drainage density**

The drainage density is the sum of all stream lengths in a drainage basin divided by the total area of the basin. The structural analysis of a drainage network helps to identify the groundwater recharge zone, and the quality of drainage

system relies on a significant index on percolation rate (Yeh et al. 2016). The drainage density is significantly correlated with the groundwater recharge, higher the drainage density refers to the high level of groundwater recharge (Yeh et al. 2016). The drainage density map (Fig. 3c) is extracted from the ASTER DEM in ArcGIS. In this study, higher the weight attributed to high drainage density and vice versa.

## Rainfall

Rainfall is one of the essential weather variables in respect to the delineation of groundwater potentiality zone. Therefore, it is necessary to understand the spatio-temporal phenomena of rains for the study of water resources. The rainfall data were acquired from the meteorological substation in Asansol Municipality. The average annual rainfall of AUA is around 1200–1400 mm and 80–85% of the total rainfall happens during July–September due to south-west Monsoon. The eastern and western part of AUA receives 1200–1400 mm/year rainfall (Fig. 3g) and central part of AUA receives > 1400 mm/year rainfall. This little difference of rainfall around the whole study area has no major influence on the variability of the groundwater potentiality zone. However, rainfall is still an important controlling factor, because rainfall is input on surface water storage and created a balance among all components of hydrological cycle.

## Soil

The availability of groundwater is highly influenced by the infiltration capacity of the topsoil of any region. Soil porosity and permeability are directly controlled by the particle size of the soil. Therefore, the characteristics of soil is an essential controlling factor for delineating the GPZ. The soil map (Fig. 3e) of AUA is collected from the National Bureau of Soil Survey and Land Use Planning. The different types of soil are available in this study area, e.g., loamy soil covers 0.81% of the total area, sandy loam covers 27.16%, sandy loam-gravelly sandy loam 0.16%, and sandy clay loamy covers 71.87% of the total area. The porosity and permeability are higher in sandy and gravelly sandy loam soil and much lower in case of clay soil. The characteristics of the soil found in this study area are more or less similar. However, the weight assigned for GPZ is higher for courser grain and less weight is assigned for finer grain soil.

## Lithology

Lithological rock types exposed to the surface has a significant impact on groundwater recharge. In this study, the lithological map (Fig. 3f) has been collected from Geological Survey of India (GSI). This map illustrates five classes of lithological units, e.g. flood plain of Damodar River, toe

slope, alluvium plain, gently sloping land, moderately sloping land. The flood plain of Damodar River and alluvium plain has the highest water holding capacity as compared to other lithological units.

## Statistical methods

### Fuzzy analytic hierarchy process (FAHP)

The analytical hierarchy process (AHP) is very useful for the multi-parametric evaluation (Saaty 1980) (Table 2). FAHP is the analytical method which is very useful to encounter the unstructured issues regarding geomorphological, socio-economic, and environment (Özdağoğlu and Özdağoğlu 2007). Moreover, fuzzy AHP is one of the hierarchical structures which envisages pairwise comparison of thematic layers with triangle fuzzy number (TFN) and it provides more accurate results compared to the decision-making traditional method AHP (Boughariou et al. 2021).

FAHP is widely used in physical and environmental fields to analyse environmental vulnerability, flood susceptibility, and groundwater potentiality mapping (Şener et al. 2018). There are several steps to delineate the groundwater potential using FAHP as follows:

The normalised fuzzy value can be calculated as

$$S_i = \sum_{j=1}^m U_{ki}^j \otimes \left[ \sum_{i=1}^n \sum_{j=1}^m U_{ki}^j \right]^{-1} \quad (1)$$

$$V(U_2 \geq U_1) = \sup [\min (\mu_{U_1}(x), \mu_{U_2}(y))] \quad (2)$$

where triangular fuzzy number of  $U_1 = (x_1, y_1, z_1)$  and  $U_2 = (x_2, y_2, z_2)$ .

Then, the chance of convex fuzzy number of  $V$  can be equated as

**Table 2** Characterization of Saaty's scale and triangular fuzzy scale

Characteristics	Saaty's scale	Fuzzy scale	Reciprocal of the fuzzy scale
Equal importance	1	(1,1,1)	(1,1,1)
Moderate importance	3	(1/2,1,3/2)	(3/2,1,2)
Strong importance	5	(1,3/2,2)	(1/2,2/3,1)
Very strong importance	7	(2,5/2,3)	(1/3,2/5,1/2)
Extreme importance	9	(5/2,3,7/2)	(2/7,1/3,2/5)
Intermediate values between adjacent judgements for Saaty's scale 2, 4, 6, 8			

Less importance < -(1/9-1/8-1/7-1/6-1/5-1/4-1/3-1/2-1-2-3-4-5-6-7-8-9) - > More importance

$$V(U \geq U_1, U_2, \dots, U_i = V[(U \geq U_1) \text{ and } (U \geq U_2) \dots \text{ and } (U \geq U_i)]), \tag{3}$$

$$d(A_i) = \min V(S_1 \geq S_2) \tag{4}$$

where  $i = 1, 2, \dots, i$ .

For normalisation of the fuzzy vector

$$W = (d(A_1), d(A_2), \dots, \dots, d(A_n))^t \tag{5}$$

where  $W$  is the non-fuzzy number.

**Frequency ratio (FR)**

Frequency ratio (FR) model is one of the bivariate statistical method that helps to measure the probability between dependent variables and independent variables of the groundwater potential zones (Balamurugan et al. 2017; Boughariou et al. 2021). In this study, groundwater conditioning factors are considered as independent variables and bore well data are considered as dependent variable. The FR can be calculated as follows:

$$FR = \frac{W/BW}{P/TP} \tag{6}$$

where  $W$  denotes the number of pixels of the bore well locations for each conditioning factor;  $BW$  denotes the number of total bore well pixels in study area;  $P$  represents the number of pixels of each class of the conditioning factor;  $TP$  denotes the number of total pixels in the study area. In FR calculation, the FR model value is obtained from the thematic layers of the conditioning factors that determine the groundwater potentiality (Balamurugan et al. 2017).

**Bayesian weights of evidence (BWOE)**

Bayesian weights of evidence (BWOE) model is a widely accepted method to calculate the groundwater potentiality (Lee et al. 2012; Kordestani et al. 2019; Boughariou et al. 2021). Based on relative weightage of the conditioning factors, BWOE model is calculated in a study area. BWOE can be expressed as follows:

$$W^+ = Ln \frac{P\left(\frac{B}{A}\right)}{P\left(\frac{B'}{A'}\right)} \tag{7}$$

$$W^- = Ln \frac{P\left(\frac{B}{A}\right)}{P\left(\frac{B'}{A'}\right)} \tag{8}$$

where  $W^+$  and  $W^-$  denote the positive and negative weights of the conditioning factors;  $P$  is the probability,  $B$  stands for conditioning factor,  $B'$  stands for absence of conditioning factors,  $A$  stands for bore well data and  $A'$  stands for absence of bore well data.

Then, the standard deviation (SD) of the contrast value can be calculated as follows:

$$SD_c = \sqrt{((S^2(W^+) + S^2(W^-)))} \tag{9}$$

where  $S^2$  denotes the influencing weight of the conditioning factors (Zeinivand and Nejad, 2018).

The standardised contrast  $\tau$  is considered as measure of confidence can be calculated as follows:

$$\tau = \left(\frac{C}{SD_c}\right) \tag{10}$$

After assigning all the conditioning parameters with the bore well data, the value of  $W^+$ ,  $W^-$ ,  $SD_c$ , and  $\tau$  has been calculated.

**Delineation of the GPZ**

**Delineation of groundwater using FAHP**

All the thematic layers are integrated with ArcGIS to generate groundwater potential index (GPI), to evaluate the groundwater potentiality zone (GPZ). The GPI has been computed by using the weighted linear combination method (Malczewski 1999; Mallick and Rudra 2021a, b) as follows:

$$GPI = \sum_{w=1}^m \sum_{i=1}^n (w_i \times x_j) \tag{11}$$

where  $w_i$  is the normalized weight of the  $i$ th thematic layer,  $x_j$  is the rank value of each class with respect to the  $j$  layer,  $m$  is the total number of themes, and  $n$  is the total number of classes in a theme. The GPZ for each factor is calculated using FAHP Eq. 12:

$$GPZ = EwEr + SLwSLr + SwSr + DDwDDR + LULCwLULCr + PwPr + LDwLDr + LwLr \tag{12}$$

where  $w$  and  $r$  represent the normalized weight index and rating of FAHP of the individual classes, respectively.  $E$  is the DEM,  $SL$  denotes slope,  $S$  represents the distribution of soil,  $DD$  represents drainage density,  $LULC$  is denoted land use land cover of the study area,  $P$  indicates volume of rainfall,  $LD$  is the lineament density, and  $L$  represents lithological condition of the study area.

## Delineation of groundwater using FR

Contrasting the FAHP, in FR, the weightage of each class is not put based on the properties of the conditioning factor but given in the form of spatial occurrence of the wells in each class. Similarly, the FR is calculated for all the conditioning factors. Finally, the GPI has been computed using Eq. 13:

$$GPI = Fr_1 + Fr_2 + \dots + Fr_n \quad (13)$$

where FR is the final weight of the conditioning factors. Then, GPZ is calculated based on frequency ratio-based GPI value of each conditioning factors as follows (Eq. 14):

$$GPZ = \sum (E_{FR} + SL_{FR} + S_{FR} + D_{FR} + LULC_{FR} + P_{FR} + LD_{FR} + L_{FR}) \quad (14)$$

where FR represents the weights of frequency ratio of the individual classes. E is the DEM, SL denotes slope, S represents the distribution of soil, DD represents drainage density, LULC denotes land use land cover of the study area, P indicates volume of rainfall, LD is the lineament density and L represents lithological condition of the study area.

## Delineation of groundwater using BWOE

BWOE is similar like FR; it is calculated and mapped according to the  $\tau$  values using Eq. 15:

$$GPI = \tau_1 + \tau_2 + \dots + \tau_n \quad (15)$$

where  $\tau$  is the final weight that comes through the calculation of  $W+$ ,  $W-$ ,  $C$ , and  $SD_c$ . Then, the GPZ is calculated according to this GPI value as follows (Eq. 16):

$$GPZ = \sum (E\tau + SL\tau + S\tau + D\tau + LULC\tau + P\tau + LD\tau + L\tau) \quad (16)$$

where E is the DEM, SL denotes slope, S represents the distribution of soil, DD represents drainage density, LULC denotes land use land cover of the study area, P indicates volume of rainfall, LD is the lineament density and L represents the lithological condition of the study area.

## Results

### FAHP

The thematic layers of conditioning factors were classified and rank was attributed to each class using Saaty's scale (Table 3) to establish the Fuzzy AHP-based groundwater potentiality map. The rank for DEM classes is decreasing following the numerical values of the thematic layer. For the lowest altitude (43–93 m.), the rank is 5; for the intermediate altitude, classes are given the rank 4, 3, and 2,

respectively, while the highest altitude (137–209 m.) class has the lowest rank 1. The rating of slope classes also has decreasing rank while the value of slope is increasing, and the highest rank (5) is attributed to the lowest slope value (0–6), whereas the lowest rank (1) is given to the highest slope value (> 24). The presence of lineaments influences the infiltration rate. Therefore, highest rank (5) is given to highest class (0.85–1.43) and rank 1 is provided for the lowest class (0–0.13). The characteristics of soil also regulate the infiltration rate. Here, highest (5) and lowest rank (2) are assigned to loamy and sandy loam- gravelly sandy loam soil. The rating for lithological unit is provided based on

the conductivity. For lithological class, highest rank (5) is given to Flood plain of Damodar River and lowest rank (2) is assigned for moderately sloping land. The amount of rainfall has an important role in groundwater recharge. In this study, two rainfall zones have been found and highest rank is given to 1400 mm/year and the lowest rank for 1200 mm/year. The rate for the LULC class has been assigned based on the infiltration capacity of each class. The highest rank (5) is given for water bodies, rank 4 for vegetation cover and agricultural field, rank 3 for dry/barren land, and rank 2 is assigned for built-up and industrial areas.

The FAHP is used to compare the eight thematic layers and normalised weights have been calculated (Table 3). As a result, the highest weight is attributed to lineament density (0.18), and the lowest weight is 0.08 for DEM parameter. The GPZ map has been generated by overlaying a thematic map based on the FAHP weights. The GPZ map (Fig. 4) obtained using FAHP model is specified four groundwater potential zones, like very high zone, covering 7.43% to the total area of AUA and found along Damodar Riverbank, a high zone covering 34.60% area, moderate zone (37.08% area) and low potential zone covering (20.90% area) (Table 5).

### FR

The groundwater potentiality zone estimation using FR model is very significant. This model executed the GPZ through correlation between conditioning factors and location of bore wells. Moreover, higher correlation value indicates the greater groundwater potential and vice versa (Manap et al. 2014). In this study, eight conditioning factors (Fig. 3) and twelve bore wells (WRIS) have been used to create GPZ map. The correlation results (Table 4) of FR model depict that lower slope per cent (0–6) is indicated by the higher value of FR (2.253), while the absent of wells in higher the slope per cent (> 24) area



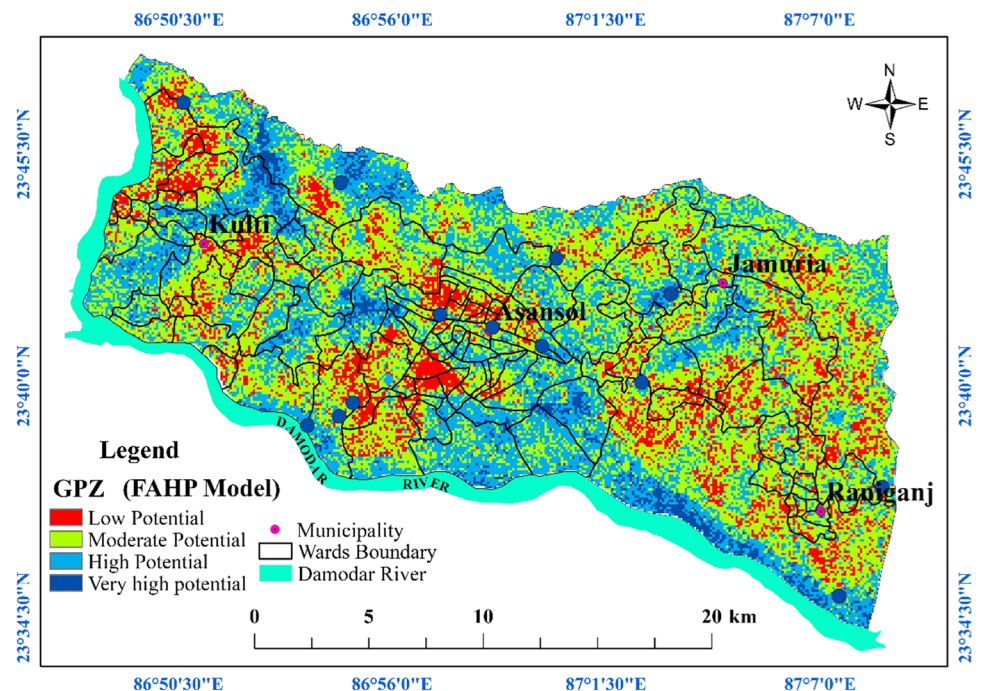
**Table 3** Different factors and classes with relative weighted index (Wi) of eight thematic layers for GPZ

Factors	Class/value	Potentiality for groundwater storage	Fuzzy AHP rating	Weighted index (Wi)
DEM (m)	43–93	Very good	5	0.08
	93–108	Good	4	
	108–122	Moderate	3	
	122–137	Poor	2	
	137–209	Very poor	1	
Slope (%)	0–6	Very good	5	0.10
	6–12	Good	4	
	12–18	Moderate	3	
	18–24	Poor	2	
	> 24	Very poor	1	
Drainage density (km/sq.km)	0.00171–0.0030	Very good	5	0.15
	0.00121–0.00171	Good	4	
	0.00081–0.00121	Moderate	3	
	0.00041–0.00081	Poor	2	
	0–0.00041	Very poor	1	
Lineaments (km/sq.km)	0.85–1.43	Very good	5	0.18
	0.58–0.85	Good	4	
	0.35–0.58	Moderate	3	
	0.13–0.35	Poor	2	
	0–0.13	Very poor	1	
Soil	Loamy	Very good	5	0.11
	Sandy loam	Good	4	
	Sandy loam- Gravelly sandy Loam	Poor	2	
	Sandy clay loam	Moderate	3	
Lithology	Flood plain of Damodar river	Very good	5	0.12
	Toe slope	Moderate	3	
	Alluvium plain	Good	4	
	Gently sloping land	Moderate	3	
	Moderately sloping land	Poor	2	
Rainfall (mm)	1200–1400	Good	4	0.14
	> 1400	Very good	5	
LULC	Built-up area	Poor	2	0.12
	Agricultural land	Good	4	
	vegetation cover	Good	4	
	Water bodies	Very good	5	
	Dry/Barren land	Moderate	3	
	Mining & Industrial area	Poor	2	

is indicated lower FR (0.00) reflecting the low groundwater potential. Meanwhile, higher value of lineaments density (0.85–1.43) shows high FR (9.328) value which indicates the greater chance to groundwater potential while low FR value (0.522) was found for the lineaments class 0.35–0.58. For lithological conditions, the result shows that the alluvium plain has the greater ability to groundwater potential with FR value (1.951). The soil characteristics are also significant for delineating GPZ. According to FR model, the sandy loam soil (FR = 4.149) has more

groundwater potential than other soil found in this region. The amount of annual rainfall is also very significant for groundwater recharge. Here, two different rainfall zones have been found, i.e. > 1400 mm/year with FR value 1.457 and 1200–1400 mm/year with FR value 0.389. Finally, the impact of urbanisation on groundwater potentiality is highly influenced by LULC classes. In this study, water body contributed the high potential ability with 9.923 while mining/industrial area and vegetation cover area found insignificant FR values because FR is analysed by

**Fig. 4** Groundwater potentiality analysis using Fuzzy AHP method



conditioning factor and bore wells data. Due to lack of bore wells data of these classes, the result indicated the low FR value while vegetation cover always greatly influenced the infiltration rate. The GPZ map (Fig. 5) obtained using FR model is specified four groundwater potential zones like very high zone, covering 11.62% to the total area of AUA and found along Damodar river bank and south-eastern part; high zone (32.45% area); moderate zone (33.84% area) and low potential zone (22.08% area) which found in the built-up and industrial areas (Table 5).

## BWOE

The groundwater potentiality zone estimation using BWOE model (Fig. 6) is also useful for this study. According to BWOE ( $\tau$ ) values (Table 4), it is noted that for the lineament, the highest  $\tau$  value is given which indicates a high groundwater potentiality. Then, rainfall, drainage density, lithology thematic maps are given next level of  $\tau$  value. Similarly, the LULC (specifically vegetation and agricultural land) has been given a positive standard value. For DEM, highest weight of  $\tau$  is given to the lowest altitude in the Damodar riverbank area. The lowest weight of DD has also a higher value of  $\tau$ , while the highest value of this parameter is detected in the highest class of lineament. For BWOE model, the quintile method was also adopted to classify the groundwater potential map into three classes: low, medium, and high. According to the final GPZ map, the low GPZ is found mostly on the Damodar riverbank

area. The delineation of the BWOE-based GPZ map shows a similar surface cover for the high and moderate groundwater potential. The low GPZ class covered slightly higher area (38.33%) than the high and moderate potential zones (Table 5).

## Validation of GPZ

The FAHP, FR, and BWOE models have been validated through receiver operating characteristics (ROC) curve. The area under the ROC curve (AUC) defines the prediction or classification accuracy (Boughariou et al. 2021). In this study, we have run and validated three models based on the classification result of the GPZ. AUC value is ranged between 0 and 1. If the value is given below 0.5, then it indicates that the result of the model is not suitable, and it needs to classify once again and close to 1 implies that the result is well delineated (Mallick et al. 2021b).

The ROC curves of the GPZ maps were generated for the validation of FAHP, FR, and BWOE methods (Fig. 7). The result demonstrating that the outcome of FR method (AUC = 96.4%) is well obtained for GPZ in comparison to the both BWOE (AUC = 83.8%) and FAHP method (AUC = 82.9%). However, all the obtained results were validated and well delineated (Mallick and Rudra 2021a). But, it can be stated that the FR is better representative for this study area to denote that the spatial distribution of the GPZ with respect to the fuzzy AHP and BWOE methods. Therefore, this

**Table 4** Spatial relationship between wells locations and conditioning factors using FR and BWOE models

Thematic Layers	Attribute details	No of pixel in a class	% of pixel in a class	No of pixel of wells	% of pixel of wells	Frequency ratio	W+	W-	C	S(C)	$\tau$ (C/S)
DEM (m)	43–93	88,688	17.29	2	16.67	0.964	2.881	-0.416	3.297	0.718	4.594
	93–108	112,731	21.98	3	25	1.137	2.716	-0.566	3.282	0.589	5.571
Slope (%)	108–122	134,948	26.32	5	41.67	1.583	2.385	-0.720	3.105	0.461	6.736
	122–137	102,532	19.99	2	16.67	0.834	3.026	-0.505	3.531	0.718	4.920
	137–209	73,900	14.41	0	0	0.000	3.392	-0.339	3.731	1.010	3.694
	0–6	132,779	25.89	7	58.33	2.253	2.032	-0.681	2.713	0.394	6.891
	6–12	169,084	32.97	3	25	0.758	3.121	-1.089	4.210	0.589	7.148
Drainage density (km/sq.km)	12–18	110,232	21.5	1	8.33	0.387	3.792	-0.568	4.360	0.199	-0.03
	18–24	71,793	14	1	8.33	0.595	3.363	-0.327	3.690	0.206	1.470
	> 24	28,911	5.64	0	0	0.000	2.454	-0.112	2.566	0.349	-0.31
	0.00171–0.0030	49,200	9.59	3	25	2.607	1.887	-0.188	2.075	1.005	-1.82
	0.00121–0.00171	100,233	19.55	2	16.67	0.853	3.004	-0.490	3.493	1.005	-0.57
	0.00081–0.00121	132,134	25.77	6	50	1.940	2.182	-0.686	2.868	0.099	-0.15
	0.00041–0.00081	124,139	24.21	1	8.33	0.344	3.911	-0.672	4.583	0.420	-5.68
	0–0.00041	104,492	20.38	0	0	0.000	3.739	-0.528	4.267	0.420	6.850
	0.85–1.43	13,730	2.68	3	25	9.328	0.610	-0.026	0.636	0.099	-1.13
	0.58–0.85	66,410	12.95	2	16.67	1.287	2.592	-0.287	2.879	0.260	-1.76
Soil	0.35–0.58	81,917	15.97	1	8.33	0.522	3.495	-0.385	3.880	0.207	-0.19
	0.13–0.35	66,167	12.9	1	8.33	0.646	3.282	-0.296	3.578	0.227	-0.2
	0–0.13	284,575	55.49	5	41.67	0.751	0.828	-0.070	0.898	0.245	2.980
	Loamy	63,133	12.31	0	0	0.000	3.235	-0.280	3.514	0.307	-0.31
	Sandy Loam	61,778	12.05	6	50	4.149	1.421	-0.221	1.642	0.202	3.320
	Sandy loam- Gravelly sandy loam	282,353	55.06	0	0	0.000	2.430	-0.109	2.539	0.222	0.550
	Sandy clay loam	105,535	20.58	6	50	2.430	1.957	-0.484	2.441	0.254	-0.52
	Flood plain of Damodar river	31,405	6.12	1	8.33	1.361	2.536	-0.124	2.660	1.005	-2.85
	Toe slope	199,234	38.85	2	16.67	0.429	3.691	-1.558	5.249	0.272	-4.28
	Alluvium plain	87,569	17.08	4	33.33	1.951	2.176	-0.389	2.564	0.204	3.560
Lithology	Gently sloping land	96,389	18.8	2	16.67	0.887	2.965	-0.464	3.429	0.237	0.990
	Moderately sloping land	98,202	19.15	3	25	1.305	2.578	-0.466	3.044	0.222	0.630
	1200–1400 (mm)	219,456	42.8	2	16.67	0.389	3.787	-2.053	5.840	0.222	0.630
	> 1400 mm	293,343	57.2	10	83.33	1.457	0.166	-0.020	0.186	0.230	-0.05

Table 4 (continued)

Thematic Layers	Attribute details	No of pixel in a class	% of pixel in a class	No of pixel of wells	% of pixel of wells	Frequency ratio	W+	W-	C	S(C)	$\tau$ (C/SC)
LULC	Built-up area	107,455	20.95	4	33.33	1.591	2.380	-0.518	2.898	0.249	-1.19
	Agricultural land	187,013	36.47	3	25	0.685	3.222	-1.336	4.558	0.201	2.020
	vegetation cover	37,760	7.36	0	0	0.000	2.721	-0.153	2.874	0.207	-1.96
	Water bodies	8625	1.68	2	16.67	9.923	0.551	-0.015	0.566	0.254	0.040
	Dry/Barren land	146,075	28.49	3	25	0.878	2.975	-0.842	3.817	0.510	0.200
	Mining & Industrial area	25,871	5.05	0	0	0.000	2.343	-0.099	2.441	0.099	-0.02

validation method is highly recommended for the study of the groundwater potential assessment.

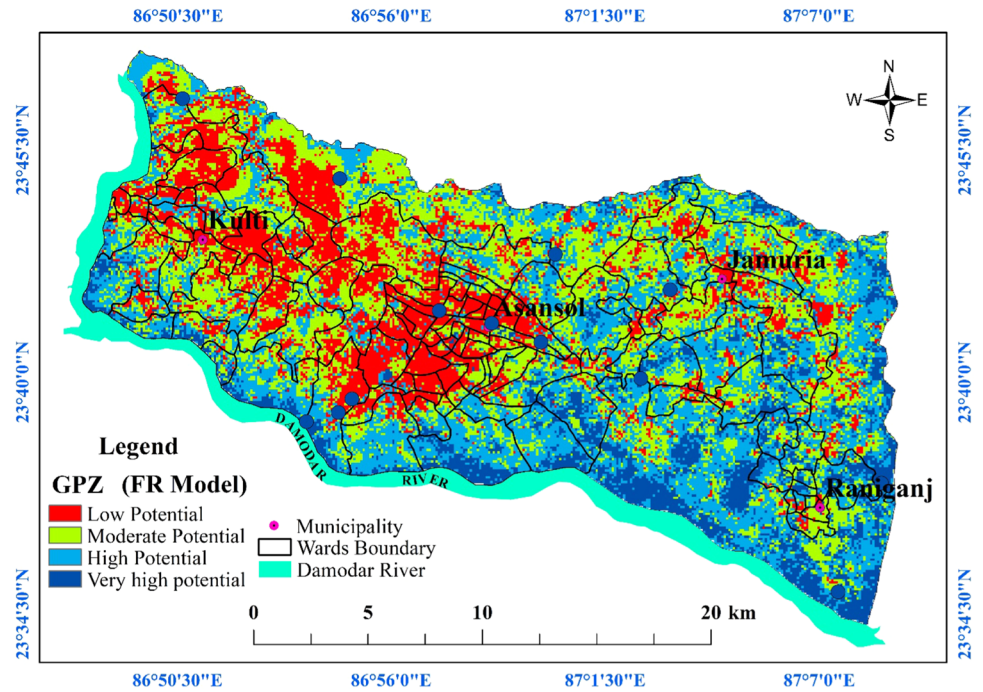
## Discussion

In this study, three models, e.g. FAHP, FR, and BWOE have been ensemble for groundwater potential zone assessment for getting better result (Nair et al. 2019; Werner et al. 2019). Eight conditioning factors of thematic maps were used as indispensable input parameters to calculate the GPZ. The GPZ value of the three models was calculated based on groundwater potential index values. The FAHP method was developed based on the literature and experts' knowledge which influenced the weightage of the conditioning factors on the study area (Mallick and Rudra 2021a). Moreover, the FR and BWOE have imposed the distribution of wells that helps to estimate the weights of each class of the conditioning factors. The output maps were classified into four zones, i.e. low potential, moderate potential, high potential, and very high potential. The results of FAHP model demonstrate that very high and low groundwater potentiality zone covers 7.43% and 20.90% to the total area, respectively. However, the maps using FR and BWOE methods revealed better representation where 11.62% and 9.13% of high groundwater potentiality including 38.88% and 22.08% of low groundwater potentiality, respectively. That means this area has high water stress than availability of potential groundwater. For these three adopted methods, the high groundwater potentiality area was located on the riverine area on the southern part of the AUA and low potentiality zones were found in the urbanised areas of the AUA. Moreover, similar method was found for groundwater potentiality validation that was area under the ROC curve (Rahmati et al. 2016).

However, it is well known that the weights of conditioning factor in groundwater potential mapping are significantly influenced by the LULC characteristics and the lithological characterises (Naghbi et al., 2015). The findings of this study support the results of Lee et al (2012) that high lineament density locations are advantageous for groundwater potential. According to Kumar et al. (2014) and Fenta et al. (2015), since lithological character and lineament density facilitate percolation and hence improve groundwater recharge. The groundwater potential increases from 1200 to 1400 mm in case of rainfall and then steadily decreases from 1400 mm onward. This could be attributed to a decrease in impermeable surface infiltration in the upland area, as well as geomorphological and topographical factors that lead to excessive runoff (Pradhan, 2009). Nevertheless, analysis of GPZ result is also helpful to identify the future urban land use development area and to maintain the urban resilience (Mallick 2021).



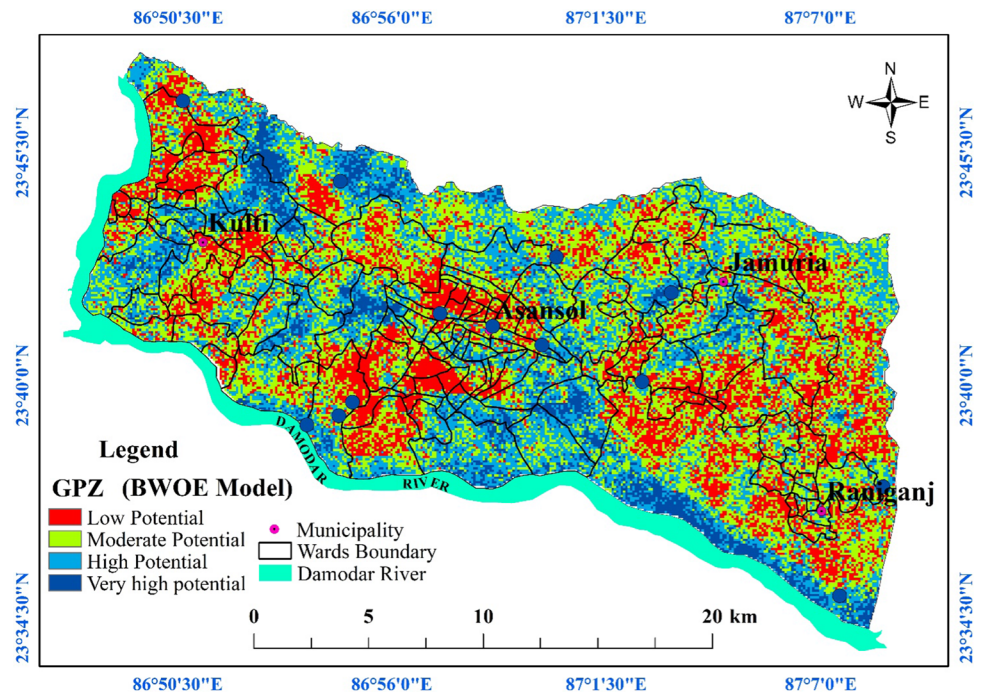
**Fig. 5** Groundwater potentiality analysis using FR method



**Table 5** Groundwater potential zonation derived from FAHP, FR and BWOE frequency ratio methods

GPZ	BWOE model	FR model		FAHP model		
	area (km <sup>2</sup> )	% of Area	Area (km <sup>2</sup> )	% of area	Area (km <sup>2</sup> )	% of area
Low	179.31	38.88	101.84	22.08	96.38	20.90
Moderate	127.87	27.73	156.09	33.84	170.99	37.08
High	111.9	24.26	149.66	32.45	159.57	34.60
Very high	42.12	9.13	53.61	11.62	34.26	7.43

**Fig. 6** Groundwater potentiality analysis using BWOE Model



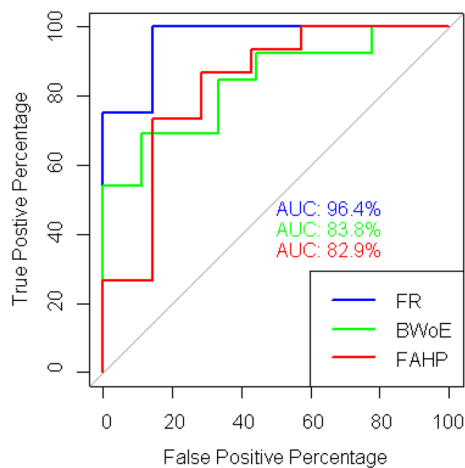


**Fig. 7** Receiver operating characteristics (ROC) curves for FAHP, FR, and BWOE methods

## Conclusion and policy recommendation

Asansol urban area is a rapidly rising urban agglomeration in West Bengal, India. The WWF-India reported that the 30 cities in India will face a grave water risk by 2050 due to sharp increase in population. The Dhanbad city in Bihar is in this list, which is located only 63.5 km away from Asansol region. In future, AUA might be facing the same crisis because both cities have the same physiographic characteristics. Therefore, proper urban built-up area planning is prerequisite for sustainable urban development. This study emphasised the identification of groundwater potentiality zone for predicting built-up area development sites around the AUA. The results of this study will help the AUA and Asansol municipality for sustainable future water resource management, including regional land use planning, future wells construction, and groundwater protection. Although the shallow aquifer of AUA was over-exploited, particularly near the Damodar River area, this outcome helps them to take further necessary action in the future days. Thus, this study can be considered as a good document for decision support in water exploitation planning and water management in AUA region. However, a few steps can be taken regarding water supply and increase in groundwater recharge like supply of water to the urban dwellers from Damodar River and Maithon water reservoir after purification, implementation of rainwater harvesting projects in the urban households, etc. Additionally, there need some more inclusive innovative methods that can be demonstrated regarding better management of water resources from the over-exploitation and changing climate scenarios.

**Funding** The present research has been funded by the University Grant Commission (UGC), Govt. of India, and it is received by authors Maity, B., Mallick, S.K., and Das, P.

## Declarations

**Conflict of interest** The authors declared that there is no such conflict of interest regarding the results and data.

**Ethical approval** The authors declare that they have followed the guidelines of this journal for integrity of the scientific record.

**Open Access** This article is licensed under a Creative Commons Attribution 4.0 International License, which permits use, sharing, adaptation, distribution and reproduction in any medium or format, as long as you give appropriate credit to the original author(s) and the source, provide a link to the Creative Commons licence, and indicate if changes were made. The images or other third party material in this article are included in the article's Creative Commons licence, unless indicated otherwise in a credit line to the material. If material is not included in the article's Creative Commons licence and your intended use is not permitted by statutory regulation or exceeds the permitted use, you will need to obtain permission directly from the copyright holder. To view a copy of this licence, visit <http://creativecommons.org/licenses/by/4.0/>.

## References

- Al-Abadi AM (2015) Groundwater potential mapping at north-eastern Wasit and Missan governorates, Iraq using a data-driven weights of evidence technique in framework of GIS. *Environ Earth Sci* 74(2):1109–1124
- Al-Ruzouq R, Shanableh A, Yilmaz AG, Idris A, Mukherjee S, Khalil MA, Gibril MBA (2019) Dam site suitability mapping and analysis using an integrated GIS and machine learning approach. *Water* 11(9):1880. <https://doi.org/10.3390/w11091880>
- Aryafar A, Yousefi S, Ardejani FD (2013) The weight of interaction of mining activities: groundwater in environmental impact assessment using fuzzy analytical hierarchy process (FAHP). *Environ Earth Sci* 68(8):2313–2324
- Balamurugan G, Seshan K, Bera S (2017) Frequency ratio model for groundwater potential mapping and its sustainable management in cold desert India. *J King Saud Univ-Sci* 29:333–347. <https://doi.org/10.1016/j.jksus.2016.08.003>
- Boughariou E, Allouche N, Brahim FB, Nasri G, Bouri S (2021) Delineation of groundwater potentials of Sfax region, Tunisia, using fuzzy analytical hierarchy process, frequency ratio, and weights of evidence models. *Environ Dev Sustain*. <https://doi.org/10.1007/s10668-021-01270-x>
- Chandramouli C, & General R (2011). Census of India 2011. Provisional population totals. New Delhi: Government of India.
- Chen W, Li H, Hou E, Wang S, Wang G, Panahi M, Xiao L (2018) GIS-based groundwater potential analysis using novel ensemble weights-of-evidence with logistic regression and functional tree models. *Sci Total Environ* 634:853–867
- Das S (2019) Comparison among influencing factor, frequency ratio, and analytical hierarchy process techniques for groundwater potential zonation in Vaitarna basin, Maharashtra. *India Groundw Sustain Dev* 8:617–629. <https://doi.org/10.1016/j.gsd.2019.03.003>

- Elmahdy SI, Mohamed MM (2015) Probabilistic frequency ratio model for groundwater potential mapping in Al Jaww plain. *UAE Arabian J Geosci* 8(4):2405–2416
- Fenta AA, Kifle A, Gebreyohannes T, Hailu G (2015) Spatial analysis of groundwater potential using remote sensing and GIS-based multi-criteria evaluation in Raya Valley, northern Ethiopia. *Hydrogeol J* 23(1):195–206
- IPCC. (2001). Climate change: the scientific basis. Contribution of Working Group I to the Third Assessment Report of The Intergovernmental Panel on Climate Change;
- Jha R, Singh VP, Vatsa V (2008) Analysis of urban development of Haridwar, India, using entropy approach. *KSCE J Civ Eng* 12:281–288
- Kordestani MD, Naghibi SA, Hashemi H, Ahmadi K, Kalantar B, Pradhan B (2019) Groundwater potential mapping using a novel data-mining ensemble model. *Hydrogeol J* 27(1):211–224
- Kumar T, Gautam AK, Kumar T (2014) Appraising the accuracy of GIS-based multi-criteria decision making technique for delineation of groundwater potential zones. *Water Resour Manage* 28(13):4449–4466
- Lee S, Kim YS, Oh HJ (2012) Application of a weights-of-evidence method and GIS to regional groundwater productivity potential mapping. *J Environ Manag* 96(1):91–105
- Machiwal D, Jha MK, Mal BC (2011) Assessment of groundwater potential in a semi-arid region of India using remote sensing, GIS and MCDM techniques. *Water Resour Manage* 25(5):1359–1386
- Maity B, Mallick SK, Rudra S (2020) Spatiotemporal dynamics of urban landscape in Asansol municipal corporation, West Bengal, India: a geospatial analysis. *GeoJournal*. <https://doi.org/10.1007/s10708-020-10315-z>
- Maity B, Mallick SK, Rudra S (2021) Integration of urban expansion with hybrid road transport network development within Haldia municipality, West Bengal. *Egypt J Remote Sens Space Sci* 24(3):471–483. <https://doi.org/10.1016/j.ejrs.2020.10.005>
- Malczewski J (1999) GIS and multicriteria decision analysis. Wiley, New York, p 392
- Mallick SK (2021) Prediction-adaptation-resilience (PAR) approach—a new pathway towards future resilience and sustainable development of urban landscape. *Geog Sus* 2(2):127–133. <https://doi.org/10.1016/j.geosus.2021.06.002>
- Mallick SK, Rudra S (2021b) Land use changes and its impact on biophysical environment: Study on a river bank. *Egypt J Remote Sens Space Sci* 24(3):1037–1049. <https://doi.org/10.1016/j.ejrs.2021.11.002>
- Mallick SK, Das P, Maity B, Rudra S, Pramanik M, Pradhan B, Sahana M (2021b) Understanding future urban growth, resilience and sustainable development of small cities using prediction-adaptation-resilience (PAR) approach. *Sustain Cities Soc* 74:103196. <https://doi.org/10.1016/j.scs.2021.103196>
- Mallick, S.K., & Rudra, S. (2021a). Analysis of groundwater potentiality zones of siliguri urban agglomeration using GIS-Based Fuzzy-AHP Approach. P. K. Shit et al. (eds.), *Groundwater and Society*, 141–160. [https://doi.org/10.1007/978-3-030-64136-8\\_7](https://doi.org/10.1007/978-3-030-64136-8_7)
- Mallick J, Al-Wadi H, Rahman A, Ahmed M (2014) Landscape dynamic characteristics using satellite data for a mountainous watershed of abha, Kingdom of Saudi Arabia. *Environ Earth Sci*. <https://doi.org/10.1007/s12665-014-3408-1>
- Mallick J, Khan RA, Ahmed A, Alqadhi SD, Alsubih M, Falqi I, & Hasan MA (2019). Modeling groundwater potential zone in a semi-arid region of aseer using fuzzy-AHP and geoinformation techniques. *Water. MDPI*. 11, 2656; <https://doi.org/10.3390/w1122656>
- Mallick SK, Maity B, & Rudra S (2021a). Aquaculture-based water quality assessment and risk remediation along the Rasulpur river belt, West Bengal. P. K. Shit et al. (eds.), *Spatial Modeling and Assessment of Environmental Contaminants, Environmental Challenges and Solutions*, 213–231. [https://doi.org/10.1007/978-3-030-63422-3\\_13](https://doi.org/10.1007/978-3-030-63422-3_13).
- Manap MA, Nampak H, Pradhan B, Lee S, Sulaiman WNA, Ramli MF (2014) Application of probabilistic-based frequency ratio model in groundwater potential mapping using remote sensing data and GIS. *Arab J Geosci* 7:711–724. <https://doi.org/10.1007/s12517-012-0795-z>
- Naghbi SA, Pourghasemi HR, Pourtaghi ZS, Rezaei A (2015) Groundwater qanat potential mapping using frequency ratio and shannon's entropy models in the moghan watershed. *Iran Earth Sci Inform* 8(1):171–186. <https://doi.org/10.1007/s12145-014-0145-7>
- Nair R, Hoang TL, Laumanns M, Chen B, Cogill R, Szabo J, Walter T (2019) An ensemble prediction model for train delays. *Transp Res C Emerg Technol* 104:196–209
- Oh HJ, Kim YS, Choi JK, Park E, Lee S (2011) GIS mapping of regional probabilistic groundwater potential in the area of Pohang city. *Korea J Hydrol* 399:3–4. <https://doi.org/10.1016/j.jhydrol.2010.12.027>
- Özdağoğlu A, & Özdağoğlu G (2007). Comparison of AHP and fuzzy AHP for the multi-criteria decisionmaking processes with linguistic evaluations. *İstanbul Ticaret Üniversitesi Fen Bilimleri Dergisi Yıl*, 1 s. 65–85
- Ozdemir A (2011) GIS-based groundwater spring potential mapping in the Sultan mountains (Konya, Turkey) using frequency ratio, weights of evidence and logistic regression methods and their comparison. *J Hydrol* 411(3–4):290–308
- Pathak D (2017) Delineation of groundwater potential zone in the Indo-Gangetic plain through GIS analysis. *J Inst Sci Technol*. <https://doi.org/10.3126/jist.v22i1.17760>
- Pradhan B (2009) Groundwater potential zonation for basaltic watersheds using satellite remote sensing data and GIS techniques. *Cent Eur J Geosci* 1(1):120–129
- Rahmati O, Samani AN, Mahdavi M, Pourghasemi HR, Zeinivand H (2014) Groundwater potential mapping at Kurdistan region of Iran using analytic hierarchy process and GIS. *Arab J Geosci* 8(9):7059–7071
- Rahmati O, Samani AN, Mahdavi M, Pourghasemi HR, Zeinivand H (2015) Groundwater potential mapping at Kurdistan region of Iran using analytic hierarchy process and GIS. *Arab J Geosci* 8(9):7059–7071
- Rahmati O, Pourghasemi HR, Melesse AM (2016) Application of GIS-based data driven random forest and maximum entropy models for groundwater potential mapping: a case study at Mehran Region. *Iran Catena* 137:360–372
- Razandi Y, Pourghasemi HR, Neisani NS, Rahmati O (2015) Application of analytical hierarchy process, frequency ratio, and certainty factor models for groundwater potential mapping using GIS. *Earth Sci Inf* 8(4):867–883
- Rogers, P. (1994). Hydrology and water quality. Changes in land use and land cover: a global perspective. *Hydrology and water quality*. 4
- Saaty TL (1980) The analytic hierarchy process. McGraw-Hill, New York
- Senanayake IP, Dissanayake DMDOK, Mayadunna BB, Weerasekera WL (2016) An approach to delineate groundwater recharge potential sites in ambalantota, Sri Lanka using GIS techniques. *Geosci Front* 7(1):115–124. <https://doi.org/10.1016/j.gsf.2015.03.002>
- Şener E, Şener Ş, Davraz A (2018) Groundwater potential mapping by combining fuzzy-analytic hierarchy process and GIS in Beyşehir lake basin, Turkey. *Arab J Geosci* 11:1–21
- Shekhar S, Pandey AC (2015) Delineation of groundwater potential zone in hard rock terrain of India using remote sensing, geographical information system (GIS) and analytic hierarchy process (AHP) techniques. *Geocarto Int* 30(4):402–421

- Shikary C, & Rudra S (2020). Measuring urban land use change and sprawl using geospatial techniques: a study on Purulia municipality, West Bengal, India. *J Indian Soc Remote Sens*. <https://doi.org/10.1007/s12524-020-01212-6>
- Singh SK, Srivastava PK, Pandey AC, Gautam SK (2013) Integrated assessment of groundwater influenced by a confluence river system: concurrence with remote sensing and geochemical modelling. *Water Resour Manage* 27(12):4291–4313
- Singh LK, Jha MK, Chowdary VM (2017) Multi-criteria analysis and gis modeling for identifying prospective water harvesting and artificial recharge sites for sustainable water supply. *J Clean Prod* 142:1436–1456. <https://doi.org/10.1016/j.jclepro.2016.11.163>
- Strohschon R, Wiethoff K, Baier K, Lu L, Bercht AL, Wehrhahn R, Azzam R (2013) Land use and water quality in Guangzhou, China: a survey of ecological and social vulnerability in four urban units of the rapidly developing megacity. *Int J Environ Res* 7:343–358
- Tiwari A, Ahuja A, Vishwakarma BD, Jain K (2019) Groundwater potential zone (GWPZ) for urban development site suitability analysis in Bhopal, India. *J Indian Soc Remote Sens*. <https://doi.org/10.1007/s12524-019-01027-0>
- United Nation (UN). (2014). World urbanization prospect, department of economic and social affairs, New York
- Wakode HB, Klaus Baier K, Jha R, Azzam R (2018) Impact of urbanization on groundwater recharge and urban water balance for the city of Hyderabad, India. *Int Soil Water Conserv Res* 6:51–62. <https://doi.org/10.1016/j.iswcr.2017.10.003>
- Werner K, Verkade JS, & Pagano TC (2019). Application of hydrological forecast verification information. *Handbook of Hydro-meteorological Ensemble Forecasting*, pp. 1013–1033.
- Yeh HF, Cheng YS, Lin HI, Lee CH (2016) mapping groundwater recharge potential zone using a gis approach in hualian river. *Taiwan Sustain Environ Res* 26(1):33–43. <https://doi.org/10.1016/j.serj.2015.09.005>
- Zeinivand H, Nejad GS (2018) Application of GIS-based data-driven models for groundwater potential mapping in Kuhdasht region of Iran. *Geocarto Int* 33(6):651–666

**Publisher's note** Springer Nature remains neutral with regard to jurisdictional claims in published maps and institutional affiliations.